

1 Article

2

Electrocatalytic Performance of Carbon Supported

3

WO₃-Contained Pd-W Nanoalloys for Oxygen

4

Reduction Reaction in Alkaline Media

5 Nan Cui, Zengfeng Guo, Wenpeng Li *, Xun Xu, Hongxia Zhao, Guang Dong, Xin Han,
6 Haoquan Zhang, Shuzheng Xu, Peipei Yu7 cuinan0565@163.com(N.C.); 18753197672@163.com(Z.G.); 17854119630@163.com(X.X.); hongxiazhao@sina.com(H.Z.);
8 15275193176@163.com(G.D.); 5944585@163.com(X.H.); Z150691133361@163.com(H.Z.);
9 xsz199712@163.com(S.X.); 18340083126@163.com(P.Y.)

10 * Correspondence: liwenpeng@qlu.edu.cn or wenpengli75@163.com; Tel.: + +86-531-8963-1208

11

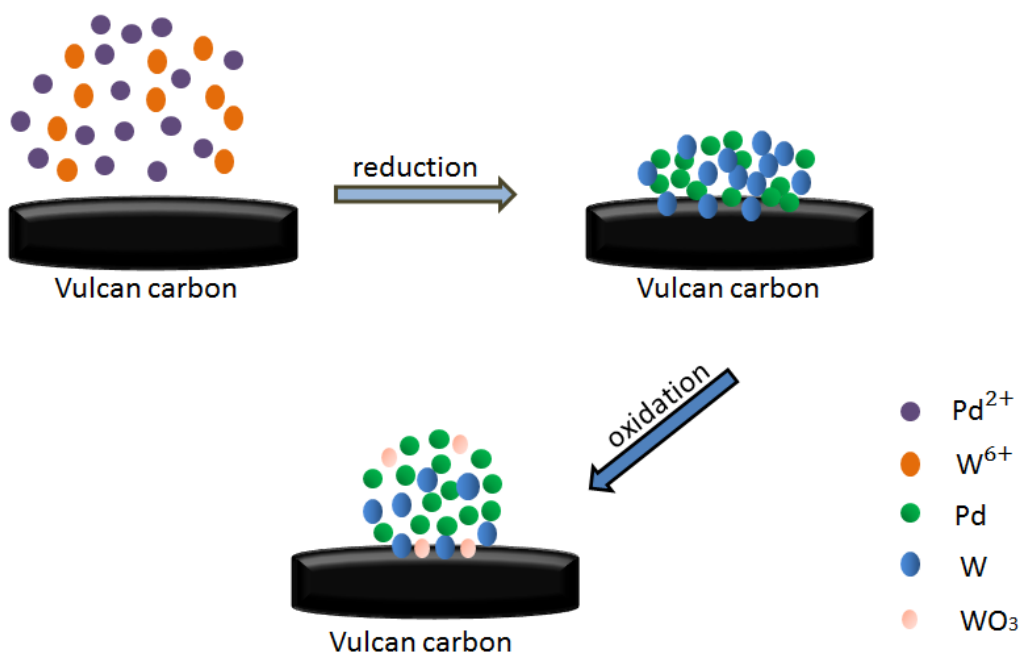
12 **Abstract:** In this paper, we first report that WO_x contained nanoalloys exhibit stable electrocatalytic
13 performance in alkaline media, though bulk WO₃ are easy to be dissolved in NaOH solutions.
14 Carbon supported oxide-rich Pd-W alloy nanoparticles (PdW/C) with different Pd:W atom ratios
15 were prepared by reduction-oxidation method. Among the catalysts, the oxide-rich Pd_{0.8}W_{0.2}/C
16 (Pd/W = 8:2, atom ratio) exhibits the highest catalytic activity for oxygen reduction reaction. The
17 X-ray photoelectron spectroscopy data shows that ~40% of Pd atoms and ~ 60% of the W atoms are
18 in their oxides form. The Pd 3d_{5/2} peaks in oxide-rich Pd-W nanoalloys are positive shift compared
19 with that of Pd/C, which indicates the electronic structure of Pd is affected by the strong interaction
20 between Pd and W/WO₃. Compare to Pd/C, the onset potential of oxygen reduction reaction at the
21 oxide-rich Pd_{0.8}W_{0.2}/C is positive shifted. The current density (mA·mg Pd⁻¹) at the oxide-rich
22 Pd_{0.8}W_{0.2}/C is ~1.6 times of that at Pd/C. The oxide-rich Pd_{0.8}W_{0.2}/C also exhibits higher catalytic
23 stability than Pd/C, which demonstrate that it is a prospective candidate for the cathode of fuel cells
24 operated with alkaline electrolyte.25 **Keywords:** WO₃; electrocatalysts; alkaline; Pd-W alloy; oxygen reduction reaction; reduction-oxidation
26 method27
2829

1. Introduction

30 The study of oxygen reduction reaction (ORR) has a long history of more than one century
31 since Grove fabricated the earliest hydrogen-oxygen fuel cell with Pt as the catalyst for ORR in 1839.
32 In recent years, the research of ORR are promoted by the increasing demand of clean energy
33 technology like fuel cells. The energy efficiency and battery voltage of the electrochemical cells are
34 obviously limited by the slow kinetics of the ORR[1,2], thus there is a great need of high efficient
35 catalysts for ORR. Various of electrocatalysts for ORR have been developed, include but not limit to
36 Pt-based catalysts[3-5], Pd-based catalysts[6,7], catalysts based on non-precious metals[8,9],
37 catalysts based on carbon nanostructure/nanocomposites[10 - 13], catalysts based on metal
38 oxides[14 , 15], catalysts based on metal-organic frameworks[16 , 17], catalysts based on metal
39 complexes[18,19], enzyme-based catalysts[20-24], metal carbides[25-28], and so on. Among the
40 catalysts for ORR, Pt-based catalysts are regarded as the most active catalysts[29]. However, the
41 scarcity of platinum limited the large scale application of Pt-based electrocatalysts. As one of the
42 alternative candidates, palladium is about 200 times abundant on the earth than platinum[30].
43 There have been some reviews about Pd-based electrocatalysts[31 - 33]The ORR [34]can be

44 performed under both acid conditions and alkaline conditions in fuel cells. It is reported that the
45 alkaline media is benefit for the kinetics of ORR[35-37]. In alkaline solutions, the oxygen can be
46 reduced through four-electron pathway or two-electron pathway[38,39]. A lot of novel Pd-based
47 electrocatalysts for ORR appears, include but not limit to carbon or metal supported Pd alloys
48 [40-42], nitrogen and sulfur co-doped carbon supported PdNi catalyst (PdNi-NS/C)[43], Pd
49 supported on TiO_2 with oxygen vacancy(Pd/ $\text{TiO}_2\text{-Vo}$) [44], PdW nanoparticles supported on
50 sulfur-doped graphene(PdW/SG)[45], PdNiCu/PdNiCo supported on nitrogen dope graphene[46],
51 PdSnCo/nitrogen-doped -graphene [47], electrochemically reduced graphene-oxide supported
52 Pd- Mn_2O_3 nanoparticles [48], AuPd@PdAu alloy nanocrystals [49],three-dimensional
53 nitrogen-doped graphene supports for palladium nanoparticles (Pd-N/3D-GNS)[50], and so on.
54 Most of the latest reports about Pd-based electrocatalysts for ORR in alkaline media mentioned
55 above are supported on graphene that had been specially treated (doping, modifying, and so on).
56 Though carbon black is the mostly used support for noble metal electrocatalysts in fuel cells,
57 Pd-based electrocatalysts supported on carbon black (C) for ORR in alkaline media is rarely
58 reported in the recent two or three years. Besides the boom of novel support materials like doped
59 graphene, one of the possible reasons is the high activity of Pd/C for ORR in alkaline media. It is
60 reported that Pd/C exhibit significantly high activity that is close to Pt/C in alkaline solutions[51,52],
61 so other electrocatalysts for ORR in alkaline media is difficult to exhibit much higher activity than
62 Pd/C. The new reports about carbon-black supported Pd based catalysts for ORR in alkaline media
63 have to face the awkward situation that compared with the ultra high active catalyst Pd/C.

64 After DFT calculations, Goddard et.al.[53]predict that Pd_3W is a prospective catalyst for ORR ,
65 which have been confirmed by our previous work $\text{Pd}_{0.7}\text{W}_{0.3}$ in acid media[54]. In this work, we
66 attempt to fabricate high performance Pd-W/C systems for ORR in alkaline media. Most of the
67 noble metal electrocatalysts used in fuel cells are in the form of naonoparticles supported on carbon.
68 Since the surface of metal nanoparticles nanoalloy are easy to be oxidized by ambient air, the effect
69 of oxides in the Pd-based catalysts for ORR in alkaline media should be discussed. The interaction
70 of metal and metal oxides in catalysts has attracted research interests for decades[55-58].It is
71 reported recently that metal and metal oxides interactions greatly affect with the catalytic
72 consequence for the electrocatalysis reactions such as oxygen reduction reaction [59]and ethanol
73 oxidation reaction[60,61]. Bulk WO_3 crystal can be dissolved in strong NaOH solutions, which
74 limited its direct application in fuel cells operated in alkaline conditions. At the beginning of this
75 work, we imagine that one of the possible solutions to solve this problem is to separate the W atoms
76 with noble metals such as Pd in the atomic scale before their oxidation. Thus the chemical bonds
77 attached to most of the W atoms are not the W-O-W bonds but Pd-W metallic bonds. The Pd-W
78 bonds is more stable than W-O-W bonds in alkaline solutions. According to Monte Carlo simulation
79 [62,63], alloy clusters at the surface of nano-materials sometimes exhibit higher stability. As
80 mentioned above, we have studied the $\text{Pd}_{0.7}\text{W}_{0.3}$ catalyst for ORR in acid media[64]. Though some of
81 the W dealloyed from the surface of $\text{Pd}_{0.7}\text{W}_{0.3}$ alloy during the ORR in acid media, the
82 electrocatalytic performance of $\text{Pd}_{0.7}\text{W}_{0.3}$ catalyst kept stable. Thus we suppose that even if a part of
83 W/WO_x leak out, the catalytic activity of the catalyst will not decay rapidly. In this paper, we
84 fabricate WO_x-contained Pd-W nanoalloys with the reduction-oxidation method (Scheme 1.). The
85 onset potential of ORR at the as prepared oxide-rich $\text{Pd}_{0.8}\text{W}_{0.2}/\text{C}$ (Pd/W=8:2, metal atomic ratio) is
86 close to the Pd/C and Pt/C fabricate with chemical reduction method[65]. The ORR stability and
87 current density (mA·mg Pd⁻¹) of the oxide-rich $\text{Pd}_{0.8}\text{W}_{0.2}/\text{C}$ is higher than that of Pd/C, which
88 indicates that the oxide-rich $\text{Pd}_{0.8}\text{W}_{0.2}/\text{C}$ is a prospective candidate for the cathode of the fuel cells
89 operated in alkaline conditions.

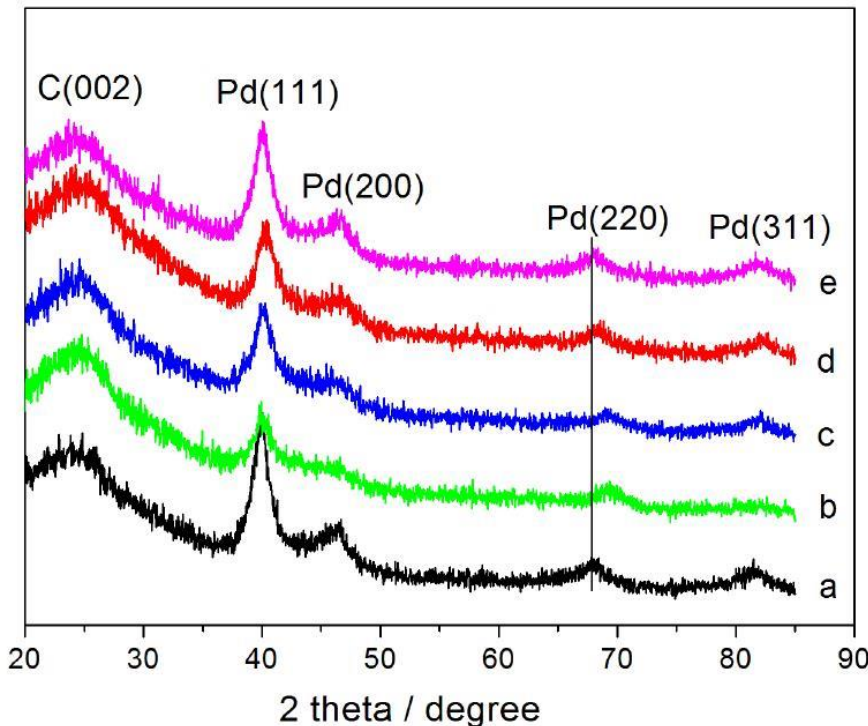


90
91 **Scheme 1.** Schematic illustration of the formation of catalyst. Dimensions are not in scales

92 **2. Results and Discussion**

93 **2.1. Characterization of oxide-rich PdW/C catalysts**

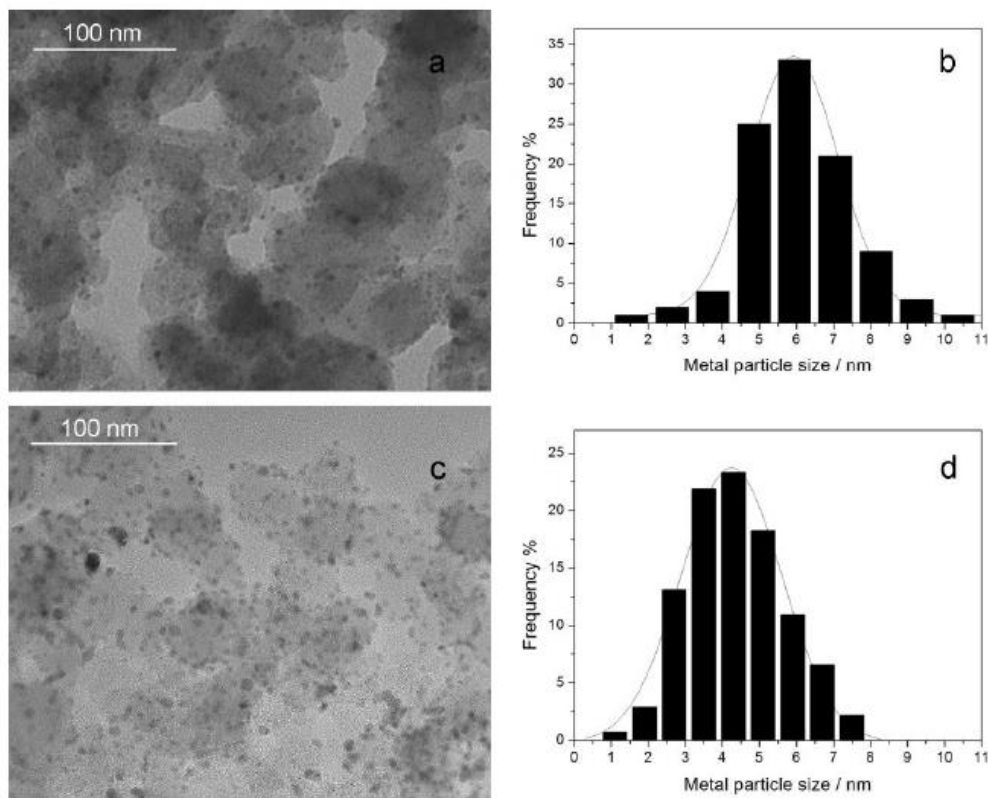
94 The X-ray diffraction (XRD) patterns of Pd/C (a), oxide-rich Pd_{0.6}W_{0.4}/C (b), Pd_{0.7}W_{0.3}/C (c),
95 Pd_{0.8}W_{0.2}/C (d), Pd_{0.9}W_{0.1}/C (e) are shown in Figure 1. Five typical diffraction peaks of the
96 catalyst were observed at about 24.8°, 40°, 46°, 68°, 82° in the diffractogram, which correspond to
97 the Vulcan XC-72R carbon (002) crystal face, face centered cubic (FCC) metal Pd (111), (200), (220)
98 and (311) crystal plane diffraction. The XRD patterns do not show any diffraction peaks
99 corresponding to W (fcc) or WO_3 , this indicates that most of the W atoms do not exist as an
100 individual phase, but entered into the lattice of Pd crystal. The absence of peaks for tungsten also
101 appears in our previous reported $\text{Pd}_{0.7}\text{W}_{0.3}$ catalyst [64] used in acid conditions. The diffraction angle
102 of crystal plane diffraction peak of the Pd element in all the PdW/C catalysts is higher than that of
103 the corresponding Pd/C catalyst. The size of catalyst metal particles can be estimated with Scherrer's
104 equation[66]. The estimated particle size of Pd/C, Pd_{0.6}W_{0.4}/C, Pd_{0.7}W_{0.3}/C, Pd_{0.8}W_{0.2}/C and Pd_{0.9}W_{0.1}/C
105 were 5.6 nm, 4.8 nm, 4.5 nm, 4.3 nm and 5.2 nm. The particle size of the oxide-rich Pd-W/C
106 nanoparticles is smaller than that of Pd/C



107

108 **Figure 1.** XRD patterns of Pd/C (a), oxide-rich Pd_{0.6}W_{0.4}/C (b), oxide-rich Pd_{0.7}W_{0.3}/C (c), oxide-rich Pd_{0.8}W_{0.2}/C (d), and oxide rich Pd_{0.9}W_{0.1}/C (e).

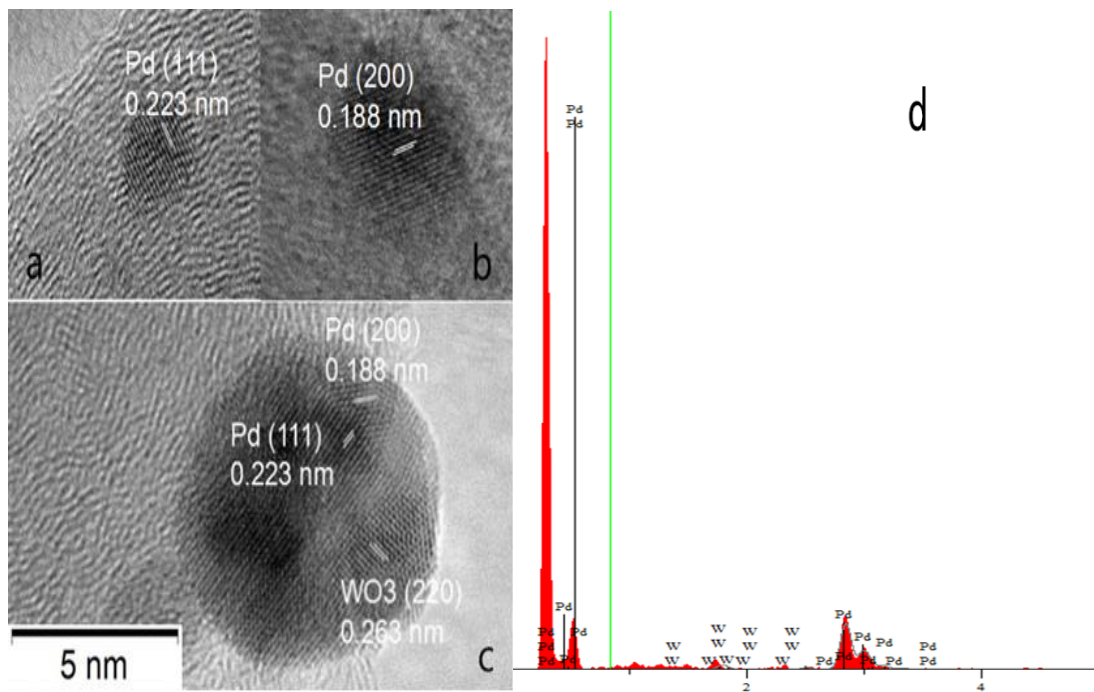
110 The morphology and particle distribution (Figure 2) of Pd/C (a, b) and oxide-rich Pd_{0.8}W_{0.2}/C (c, d) have been characterized by transmission electron microscope (TEM). The oxide-rich Pd_{0.8}W_{0.2} nanoparticles are more uniformly dispersed on the carbon surface than Pd. The average diameter of Pd nanoparticles is 5.6 nm while the average metal particle diameter of oxide-rich Pd_{0.8}W_{0.2} is 4.3 nm. Which are consistent with the XRD results. Figure 3 (a, b, c) shows the HRTEM of oxide-rich Pd_{0.8}W_{0.2}/C catalyst. The lattice spacing in Figure 3 (a, b, c) is 0.224 nm, 0.193 nm and 0.263 nm which respectively correspond to the (111), (200) crystal planes of face-centered cubic Pd and (220) plane of WO₃, respectively. The lattice fringes of WO₃ can be found in a few nanoparticles. Which support the existence of WO_x in the Pd_{0.8}W_{0.2}/C catalysts. Though there is no diffraction peaks corresponding to W in the XRD patterns mentioned above, the energy dispersive spectrum (EDS) of the as prepared oxide-rich (Figure 3d) shows the content of W in the Pd-W nanoalloys.



121

122 **Figure 2.** The morphology and particle distribution of Pd/C (a, b) and oxide-rich Pd_{0.8}W_{0.2}/C
123 (c, d) .

124



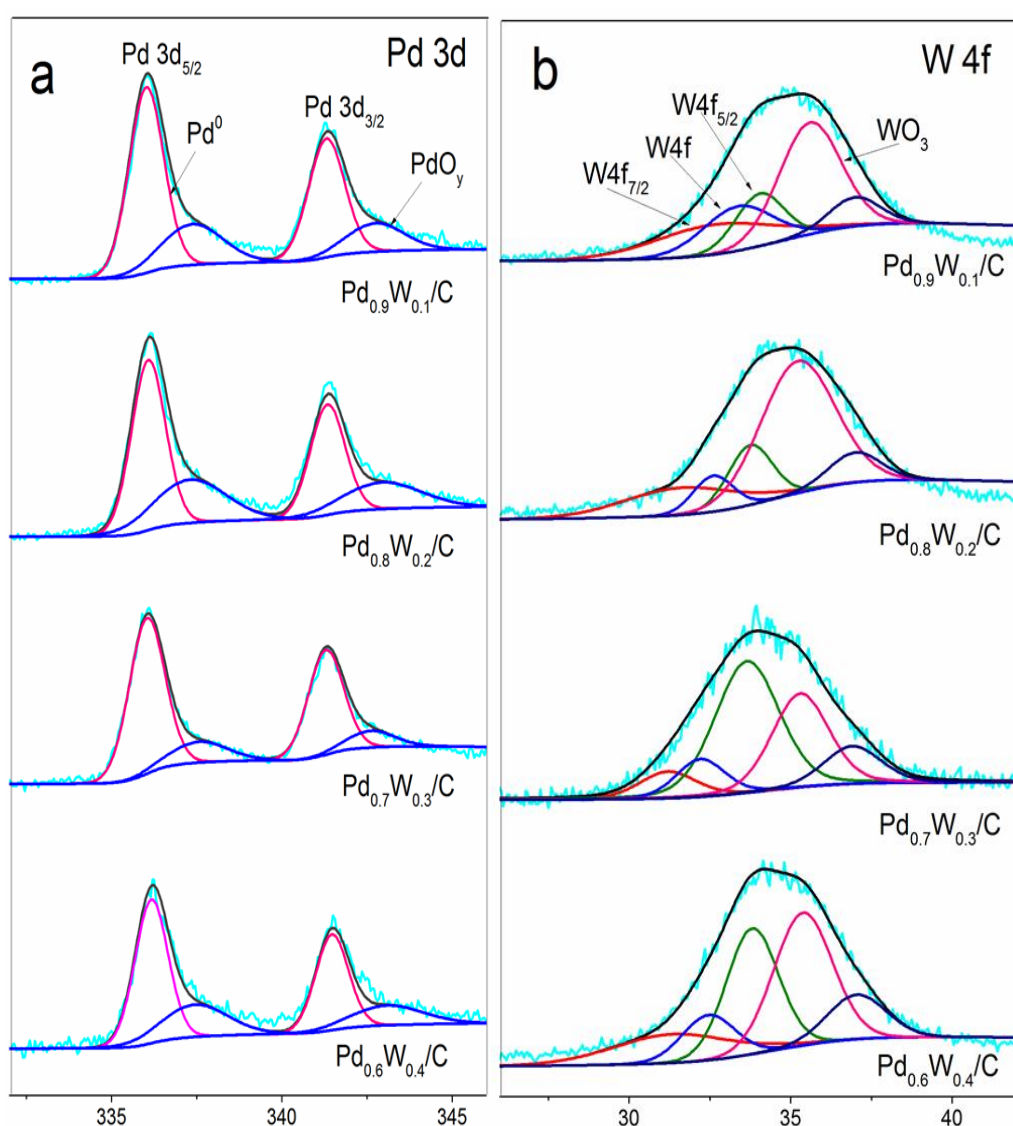
125

126 **Figure 3.** HR-TEM (a, b, c) and EDS (d) spectra of the oxide-rich Pd_{0.8}W_{0.2} / C catalyst

127

128

129 Figures 4 shows the X-ray photoelectron spectroscopy (XPS) spectra of oxide-rich $\text{Pd}_{0.6}\text{W}_{0.4}/\text{C}$,
 130 $\text{Pd}_{0.7}\text{W}_{0.3}/\text{C}$, $\text{Pd}_{0.8}\text{W}_{0.2}/\text{C}$, $\text{Pd}_{0.9}\text{W}_{0.1}/\text{C}$. The XPS spectra of Pd/C has been published in our recent
 131 works [67-69].All XPS curves were fitted using the Gaussian-Lorentzian (20%) method after
 132 subtracting the background with Shirley's method. The compositions obtained by XPS analysis is
 133 shown in Table 1. The surface composition ratios of the Pd : W elements in oxide-rich $\text{Pd}_{0.6}\text{W}_{0.4}/\text{C}$,
 134 $\text{Pd}_{0.7}\text{W}_{0.3}/\text{C}$, $\text{Pd}_{0.8}\text{W}_{0.2}/\text{C}$ and $\text{Pd}_{0.9}\text{W}_{0.1}/\text{C}$ are $\text{Pd}_{0.57}\text{W}_{0.43}$ 、 $\text{Pd}_{0.70}\text{W}_{0.20}$ 、 $\text{Pd}_{0.79}\text{W}_{0.21}$ 、 $\text{Pd}_{0.87}\text{W}_{0.23}$,
 135 respectively. In Figure 4 (a), the peaks of Pd $3\text{d}_{5/2}$ and Pd $3\text{d}_{3/2}$ are corresponding to Pd and PdO_y
 136 ($0 < 2 < y$), and the Pd element is present in all the samples as Pd metal and PdO_y . The binding energy
 137 of Pd $3\text{d}_{5/2}$ peak of PdW/C catalysts shift +0.21 eV, +0.28 eV, +0.36 eV, +0.52 eV respectively
 138 compared with that of Pd/C (335.6 eV, the solid line).The positive shifts of the Pd 3d binding energy
 139 indicate the decrease of Pd 3d electronic cloud densities. Which is due to the formation of
 140 high-valency oxides. Figure 4 (b) is the peak of W 4f.



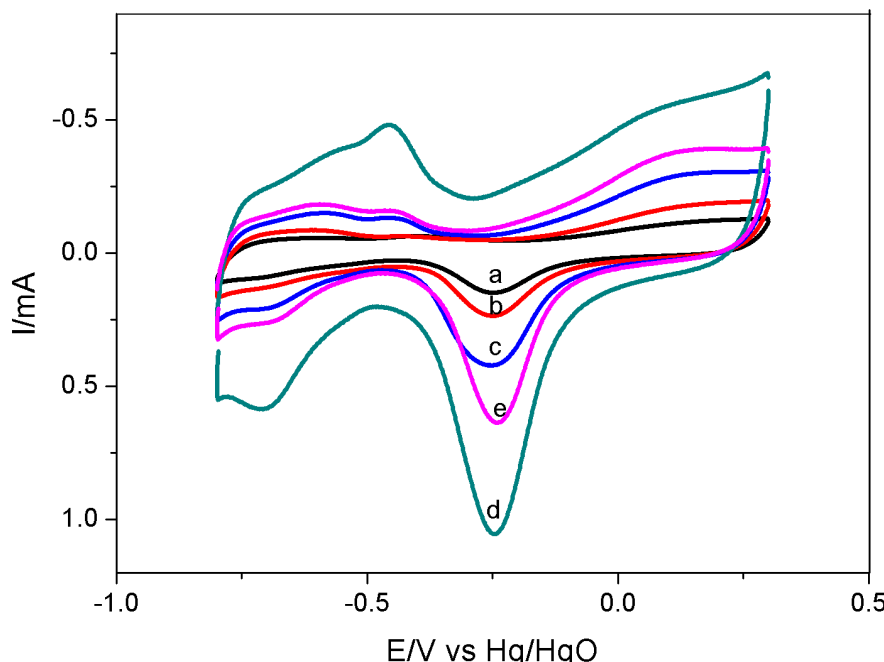
141

142 **Figure 4.** XPS spectra of oxide-rich PdW/C catalyst

143 *2.2. Electrochemical performance*

144 Figure 5 show the cyclic voltammograms (CV) of Pd/C (a), oxide-rich $\text{Pd}_{0.6}\text{W}_{0.4}/\text{C}$ (b),
 145 $\text{Pd}_{0.7}\text{W}_{0.3}/\text{C}$ (c), $\text{Pd}_{0.8}\text{W}_{0.2}$ /C (d), $\text{Pd}_{0.9}\text{W}_{0.1}/\text{C}$ (e), all the CVs were measured in 1 M NaOH

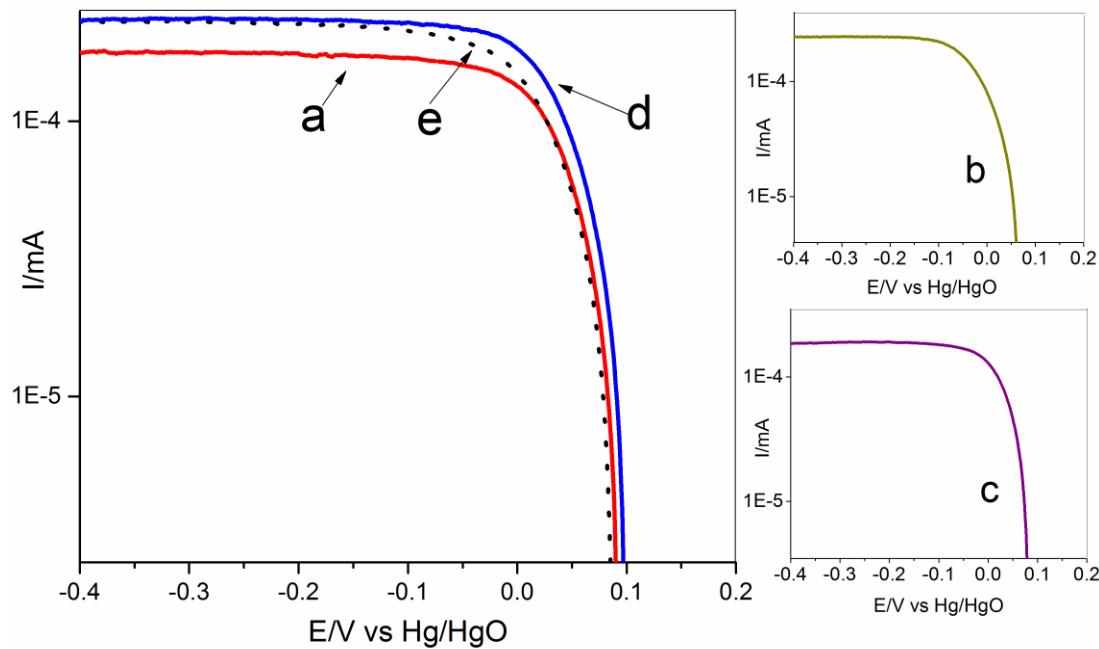
146 solution at a scan rate of $10 \text{ mV}\cdot\text{s}^{-1}$. The peak of hydrogen adsorption / desorption is at about -0.7 V.
147 The peak of OH^- adsorbed on the surface of the electrocatalysts is in the range from -0.6 to -0.4 V,
148 while the oxidation of the surface metal and the resulting reduction of the oxide are in the range
149 from -0.4 V to 0.2 V.



150

151 **Figure 5.** Cyclic voltammograms (CV) of Pd/C (a), oxide-rich $\text{Pd}_{0.6}\text{W}_{0.4}/\text{C}$ (b), oxide-rich
152 $\text{Pd}_{0.7}\text{W}_{0.3}/\text{C}$ (c), oxide-rich $\text{Pd}_{0.8}\text{W}_{0.2}/\text{C}$ (d), oxide-rich $\text{Pd}_{0.9}\text{W}_{0.1}/\text{C}$ (e). In 0.1 M NaOH solution. Scan
153 rate $10 \text{ mV}\cdot\text{s}^{-1}$

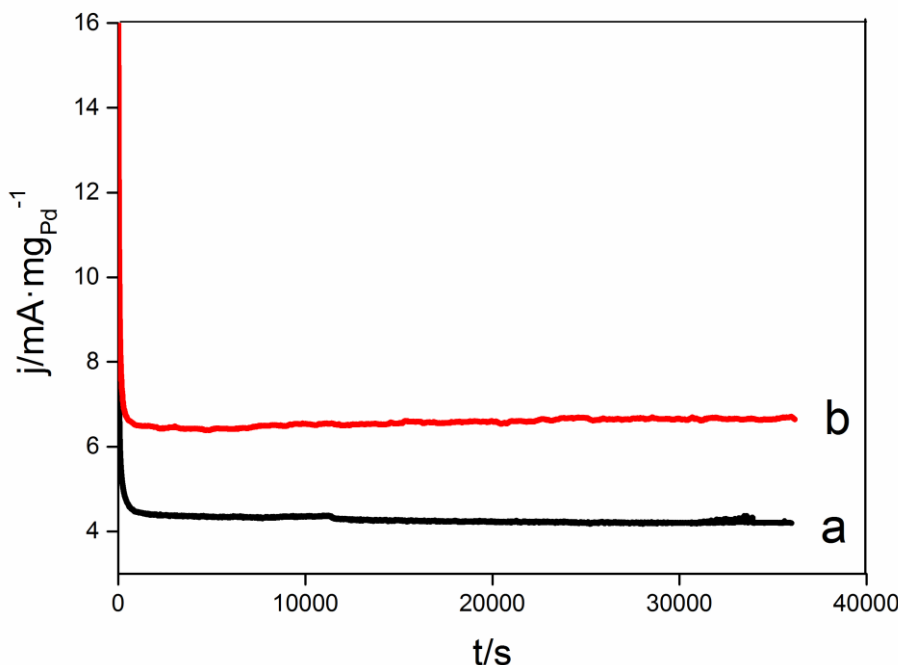
154 Figure 6 displays the linear sweep voltammetry (LSV) of Pd/C (a), oxide-rich $\text{Pd}_{0.6}\text{W}_{0.4}/\text{C}$ (b),
155 $\text{Pd}_{0.7}\text{W}_{0.3}/\text{C}$ (c), $\text{Pd}_{0.8}\text{W}_{0.2}/\text{C}$ (d), $\text{Pd}_{0.9}\text{W}_{0.1}/\text{C}$ (e) catalysts were measured in 0.1 M NaOH solution with
156 saturated O_2 at a speed of 2000 r/min and a scan rate of $1 \text{ mV}\cdot\text{s}^{-1}$. Compare to Pd/C catalyst, the
157 onset potential of oxide-rich $\text{Pd}_{0.8}\text{W}_{0.2}/\text{C}$ catalysts is positive shifted. Which is consistent to the
158 theoretic calculation results about the high activity of Pd_3W by Goddard[70] and his coworkers .



159

160 **Figure 6.** LSV of Pd/C (a), oxide-rich Pd_{0.6}W_{0.4} / C (b), oxide-rich Pd_{0.7}W_{0.3} / C (c), oxide-rich
 161 Pd_{0.8}W_{0.2}/C (d), oxide-rich Pd_{0.9}W_{0.1}/C (e) . In 0.1 M NaOH solution saturated with O₂ . Rotating
 162 speed 2000 r/min. Scan rate 1 mV·s⁻¹.

163 Electrocatalytic stability of Pd/C and oxide-rich Pd_{0.8}W_{0.2}C catalysts were characterized by
 164 chronoamperometry (Figure 7) at -0.3 V vs Hg/HgO in 0.1 M NaOH solution. At the beginning both
 165 current of Pd/C and oxide-rich Pd_{0.8}W_{0.2}/C catalyst decreased rapidly, then the current density of
 166 each catalyst was relatively stable. Obviously the oxide-rich Pd_{0.8}W_{0.2}/C catalyst exhibits higher
 167 electrocatalytic stability than Pd/C. Though the electrocatalytic stability is confirmed, it is still
 168 difficulty for us to draw a conclusion that the composition of the WO₃ contained Pd-W nanoalloys is
 169 unchanged during the ORR measurements. Some catalysts with unchanged compositions such as
 170 pure Pd[71] or pure Pt[72] sometimes exhibit poor electrocatalytic stability. The catalysts Pd_{0.7}W_{0.3}
 171 [64] for ORR in acid media exhibit high catalytic stability. However, its surface composition changed
 172 during the ORR measurement. It can be seen from figure 6 that Pd_{0.9}W_{0.1}/C also exhibit high activity.
 173 That means even if a half of the W/WO₃ dealloyed from the Pd_{0.8}W_{0.2} nanoalloys, the Pd-W catalysts
 174 still keep high activity. The current density (mA·mg Pd⁻¹) at the oxide-rich Pd_{0.8}W_{0.2}/C is more than
 175 1.6 times of that at Pd/C



176

177 **Figure 7.** Electrocatalytic stability of Pd/C (a) and oxide-rich Pd_{0.8}W_{0.2}/C (b) . In 0.1 mol/L
178 NaOH solution saturated with oxygen. Potential -0.3 V vs Hg/HgO. Rotating speed 2000 r/min.

179 **3. Materials and Methods**180 **3.1 Preparation and characterization of the catalysts**

181 PdCl₂ was purchased from Sinopharm Chemical Reagent Co.Ltd (Shanghai, China). The
182 Vulcan carbon powder XC-72R was obtained from Cabot Corporation (Cabot Corp., Billerica, MA,
183 USA). Nafion solution (5%) was obtained from DuPont (Delaware, DE, USA). All other chemicals
184 were of analytical grade and used as acquired unless otherwise noted. Triple-distilled water was
185 used through-out. The WO₃ contained Pd-W catalysts were prepared with the reduction-oxidation
186 procedures, which is schematically illustrated in Scheme 1.

187 Pd/C and PdW/C catalysts with the metal loading of 20 wt% were prepared by the NaBH₄
188 chemical reduction method (Scheme 1, step 1) we have used before [73] . PdCl₂ and Na₂WO₄ were
189 used as the precursors. Electrocatalysts with different atomic ratios are controlled by the molar ratio
190 of metal precursors. The Pd-W nanoalloys are easy to be oxide in the ambient air and formed the
191 WO₃-contained Pd-W/C catalysts (Scheme 1, step 2).

192 The X-ray diffraction analysis (XRD) was carried out by a Bruker D8 advance X-ray
193 diffractometer operating at 40 keV and 30 mA with Cu K α radiation source, $\lambda = 0.15406$ nm. The
194 TEM/HRTEM images were obtained on a JEOL JEM-2100 transmission electron microscopy . The
195 content of metal elements on the surface of the samples was analyzed by EDS. The presence of the
196 metal was excited by X-ray photoelectron spectroscopy (XPS) using Al K α X-ray radiation on an
197 ESCALAB 250 (Thermo Fisher SCIENTIFIC) spectrometer. Peak fitting using Gaussian / Lorentzian
198 (20% Gaussian) method after background subtraction using Shirley's method[74].

199 3.2 Electrochemical Measurements

200 The electrochemical measurements were performed with a CHI832B electrochemical workstation
201 (CHI Instruments, Austin, TX, USA) and a conventional three-electrode electrochemical cell. A
202 carbon-rod was used as the auxiliary electrode. Hg/HgO electrode was used as the reference
203 electrode. The working electrode was prepared with the following procedures: The glassy carbon
204 electrode (GCE, 3 mm in diameter) was carefully polished with 0.05 μ m alumina (Al_2O_3) powder,
205 and washed with the triple-distilled water before use. 10 mg of the catalyst powder in a mixture of
206 0.5 mL water and 0.5 mL ethanol was ultrasonicated for 15 min to prepare the ink of catalysts. 20 μ L
207 (2 μ L \times 10 times) of the ink was dropped on the GCE. 3 μ L of Nafion solution (5 wt%) was dropped
208 on the surface after the ink was dried in air.

209

210 4. Conclusions

211 The WO_3 contained oxide-rich Pd-W/C catalysts were successful fabricated by
212 reduction-oxidation procedures. The As prepared oxide-rich $\text{Pd}_{0.8}\text{W}_{0.2}/\text{C}$ catalysts exhibit high
213 electrocatalytic activity and stability. Which demonstrates that the as prepared oxide-rich $\text{Pd}_{0.8}\text{W}_{0.2}/\text{C}$
214 is a prospective candidate for the cathode of the fuel cells operated with alkaline electrolyte..

215 **Acknowledgments:** This work was supported by the Natural Science Foundation of Shandong Province
216 (ZR2016BM31)

217 **Author Contributions:** The corresponding author Wengpeng Li is the advisor/director of all other authors.
218 Wengpeng Li and Nan Cui conceived and designed the experiments. Nan Cui and Zengfeng Guo performed the
219 experiments; Xun Xu, Hongxia Zhao analyze the experiment data; Guang Dong, Xin Han, Haoquan
220 Zhang, Shuzheng Xu, Peipei Yu repeated the experiments to make sure the results to be repeatable; Nan Cui
221 wrote the paper

222 **Conflicts of Interest:** The authors declare no conflict of interest.

223 References

224

225

1. J. Lee, B. Jeong and J. D. Ocon, Current Applied Physics, **2013**, 13, 309–321
2. Dongyo Shin, Beomgyun Jeong, Myounghoon Choun, Joey D. Ocon and Jaeyoung Lee, Diagnosis of the measurement inconsistencies of carbon-based electrocatalysts for the oxygen reduction reaction in alkaline media, RSC Adv., **2015**, 5, 1571
3. Yan-Jie Wang, Nana Zhao Baizeng Fang, Hui Li, Xiaotao T. Bi, and Haijiang Wang, Carbon-Supported Pt-Based Alloy Electrocatalysts for the Oxygen Reduction Reaction in Polymer Electrolyte Membrane Fuel Cells: Particle Size, Shape, and Composition Manipulation and Their Impact to Activity, Chem. Rev., **2015**, 115 (9), pp 3433–3467
4. Xin Long Tian; Yang Yang Xu; Wenyu Zhang; Tian Wu; Bao Yu Xia; Xin Wang, Unsupported Platinum-Based Electrocatalysts for Oxygen Reduction Reaction, ACS Energy Letters, **2017**, 2, 2035–2043
5. Peptide templated AuPt alloyed nanoparticles as highly efficient bi-functional electrocatalysts for both oxygen reduction reaction and hydrogen evolution reaction
6. Lulu Zhang, Qiaowan Chang, Huimei Chen, Minhua Shao, Recent advances in palladium-based electrocatalysts for fuel cell reactions and hydrogen evolution reaction, Nano Energy, **2016**, 29, 198–219
7. Stefanie Kühl, Peter Strasser, Oxygen Electrocatalysis on Dealloyed Pt Nanocatalysts, Top Catal **2016** 59:1628–1637
8. Cheng Du, Xiaohui Gao, Wei Chen, Recent developments in copper-based, non-noble metal electrocatalysts for the oxygen reduction reaction, Recent developments in copper-based, non-noble metal electrocatalysts for the oxygen reduction reaction, **2016**, 37, 1049–1061
9. Varun Vij, Siraj Sultan, Ahmad M. Harzandi, Abhishek Meena, Jitendra N. Tiwari, Wang-Geun Lee, Taeseung Yoon, and Kwang S. Kim, Nickel-Based Electrocatalysts for Energy-Related Applications:

Oxygen Reduction, Oxygen Evolution, and Hydrogen Evolution Reactions, *ACS Catal.*, **2017**, 7 (10), pp 7196–7225

10. Lijun Yang, Yu Zhao, Shen Chen, Qiang Wu, Xizhang Wang, Zheng Hu, A mini review on carbon-based metal-free electrocatalysts for oxygen reduction reaction, *Chinese Journal of Catalysis*, **2013**, 34, 1986-1991

11. Gang Wu, Ana Santandreu, William Kellogg, Shiva Gupta, Ogechi Ogoke, Hanguang Zhang, Hsing-Lin Wang, Liming Dai, Carbon nanocomposite catalysts for oxygen reduction and evolution reactions: From nitrogen doping to transition-metal addition, *Nano Energy*, **2016**, 29, 83-110

12. Samaneh Shahgaldi, Jean Hamelin, Improved carbon nanostructures as a novel catalyst support in the cathode side of PEMFC: a critical review, *Carbon*, **2015**, 94, 705-728

13. Cicero W.B. Bezerra, Lei Zhang, Kunchan Lee, Hansan Liu, Aldaléa L.B. Marques, Edmar P. Marques, Haijiang Wang, Jiujun Zhang, A review of Fe–N/C and Co–N/C catalysts for the oxygen reduction reaction, *Electrochimica Acta*, **2008**, 53, 4937-4951

14. Hannah Osgood, Surya V. Devaguptapu, Hui Xu, Jaephil Cho, Gang Wu, Transition metal (Fe, Co, Ni, and Mn) oxides for oxygen reduction and evolution bifunctional catalysts in alkaline media, *Nano Today*, **2016**, 11, 601-625

15. Stoerzinger, Kelsey A., Marcel Risch, Binghong Han, and Yang Shao-Horn. "Recent Insights into Manganese Oxides in Catalyzing Oxygen Reduction Kinetics." *ACS Catalysis* 5, no. 10 (October 2, 2015): 6021–6031

16. Shaofang Fu; Chengzhou Zhu; Junhua Song; Dan Du and Yuehe Lin, Metal-Organic Framework-Derived Non-Precious Metal Nanocatalysts for Oxygen Reduction Reaction, *Advanced Energy Materials*, **2017**, 7, 1700363

17. Song, Z.; Cheng, N.; Lushington, A.; Sun, X. Recent Progress on MOF-Derived Nanomaterials as Advanced Electrocatalysts in Fuel Cells. *Catalysts* **2016**, 6, 116

18. Ja-Yeon Choi, Drew Higgins, Gaopeng Jiang, Ryan Hsu, Jinli Qiao, Zhongwei Chen, Iron-tetracyanobenzene complex derived non-precious catalyst for oxygen reduction reaction, *Electrochimica Acta*, **2015**, 162, 224-229

19. Matthew A. Thorseth, Claire E. Tornow, Edmund C.M. Tse, Andrew A. Gewirth, Cu complexes that catalyze the oxygen reduction reaction, *Coordination Chemistry Reviews*, **2013**, 257, 130-139

20. J. L. Fernández, N. Mano, A. Heller, A. J. Bard, "Optimization of "Wired" Enzyme O₂-Electroreduction Catalyst compositions by Scanning Electrochemical Microscopy" *Angew. Chem. Int. Ed.* 43, 6355-6357 **2004**

21. N. Mano, J. L. Fernández, Y. Kim, W. Shin, A. J. Bard, A. Heller, "Oxygen is Electroreduced to Water on a "Wired" Enzyme Electrode at a Lesser Overpotential than on Platinum" *J. Am. Chem. Soc.*, 125, 15290-15291 **2003**.

22. Chakraborty S; Babanova S; Rocha RC; Desiréddy A; Artyushkova K; Boncella AE; Atanassov P; Martinez JS, A Hybrid DNA-Templated Gold Nanocluster For Enhanced Enzymatic Reduction of Oxygen, *J. Am. Chem. Soc.*, **2015**, 137 (36), pp 11678–11687

23. Jonathan Husband, Michael S. Aaron, Rajneesh K. Bains, Andrew R. Lewis, Jeffrey J. Warren, Catalytic reduction of dioxygen with modified *Thermus thermophilus* cytochrome c552, *Journal of Inorganic Biochemistry*, **2016**, 157, 8-14

24. Tsujimura, Seiya; Suraniti, Emmanuel; Durand, Fabien; Mano, Nicolas, Oxygen reduction reactions of the thermostable bilirubin oxidase from *Bacillus pumilus* on mesoporous carbon-cryogel electrodes, *Electrochimica Acta*, **2014**, 117, 263-267

25. Hu Y, et al. Hollow spheres of iron carbide nanoparticles encased in graphitic layers as oxygen reduction catalysts. *Angew Chem Int Ed* **2014**;53(14):3675–679

26. Wei Wang; Shouyuan Xue; Jinmei Li; Fengxia Wang; Yumao Kang; Ziqiang Lei, Cerium carbide embedded in nitrogen-doped carbon as a highly active electrocatalyst for oxygen reduction reaction, *Journal of Power Sources*, **2017**, 359, 487-493

27. Junjie Guo; Zhe Maob; Xiaoli Yana; Rui Suc; Pengfei Guanc; Bingshe Xua; Xuefeng Zhangb; Gaowu Qinb; Stephen J. Pennycookd, Ultrasmall tungsten carbide catalysts stabilized in graphitic layers for high-performance oxygen reduction reaction, *Nano Energy*, **2016**, 28, 261-268

28. Bukola, Saheed; Merzougui, Belabbes; Akinpelu, Akeem; Zeama, Mostafa, Cobalt and Nitrogen Co-Doped Tungsten Carbide Catalyst for Oxygen Reduction and Hydrogen Evolution Reactions, *Electrochimica Acta*, **2016**, 190, 1113-1123

29. John Stacy, Yagya N. Regmi, Brian Leonard, Maohong Fan, The recent progress and future of oxygen reduction reaction catalysis: A review, *Renewable and Sustainable Energy Reviews* 69 **2017**, 401–414

30. Z. Zhang, X. Le, S. Kai, et al., *Fuel Energy Abstracts* 36, 12686 **2011**.

31. Erikson, H.; Sarapuu, A.; Solla-Gullón, J.; Tammeveski, K. *J. Electroanal. Chem.* **2016**, 780, 327-336

32. Antolini, E. *Energy Environ Sci.* **2009**, 2, 915-931

33. Kabir, S.; Serov, A., *Electrochemistry* **2017**, 14, 61-101

34. Nie, Y.; Li, L.; Wei, Z. *Chem. Soc. Rev.* **2015**, 44, 2168-2201

35. Drew Higgins, Pouyan Zamani, Aiping Yu and Zhongwei Chen, The application of graphene and its composites in oxygen reduction electrocatalysis: a perspective and review of recent progress, *Energy Environ. Sci.*, **2016**, 9, 357--390

36. Xiaoming Ge, Afriyanti Sumboja, Delvin Wuu, Tao An, Bing Li, F. W. Thomas Goh, T. S. Andy Hor, Yun Zong, and Zhaolin Liu, Oxygen Reduction in Alkaline Media: From Mechanisms to Recent Advances of Catalysts, *ACS Catal.* **2015**, 5, 4643-4667

37. Ramaswamy, N.; Mukerjee, S. *Adv. Phys. Chem.* **2012**, 2012, Article no. 491604

38. *ACS Catal.* **2015**, 5, 4643-4667

39. Lide, D. R. Eds.; CRC Press (Taylor and Francis Group): Boca Raton, FL, **2009**; Section 8, p 23

40. *Electrochem Commun* **2009**, 11, 1162-1165

41. Alexeyeva, N.; Sarapuu, A.; Tammeveski, K.; Vidal-Iglesias, F. J.; Solla-Gullón, J.; Feliu, J. M. *Electrochim. Acta* **2011**, 56, 6702-6708

42. Arenz, M.; Schmidt, T. J.; Wandelt, K.; Ross, P. N.; Markovic, N. M. *J. Phys. Chem. B* **2003**, 107, 9813-9819

43. Yongliang Li, Sen Lin, Xiangzhong Ren, Hongwei Mi, Peixin Zhang, Lingna Sun, Libo Deng, Yuan Gao, One-step rapid in-situ synthesis of nitrogen and sulfur co-doped three-dimensional honeycomb-ordered carbon supported PdNi nanoparticles as efficient electrocatalyst for oxygen reduction reaction in alkaline solution, *Electrochimica Acta*, Volume 253, 1 November **2017**, Pages 445-454

44. Jing Li, Hu Zhou, Han Zhuo, Zhongzhe Wei, Guilin Zhuang, Xing Zhong, Shengwei Deng, Xiaonian Li and Jianguo Wang, Oxygen vacancies on TiO₂ promoted the activity and stability of supported Pd nanoparticles for the oxygen reduction reaction, *J. Mater. Chem. A*, **2018**, 6, 2264-2272

45. *Electrochemistry Communications* **2016**, 68-71

46. *Electrochimica Acta*, Volume 235, 1 May **2017**, Pages 543-552

47. *Electrochimica Acta* **2017**, 36-44

48. *Applied Surface Science*, Volume 434, 15 March **2018**, Pages 905-912

49. *Journal of Energy Chemistry*, Volume 26, Issue 6, November **2017**, Pages 1153-1159

50. *ACS Catal.*, **2017**, 7 (10), pp 6609-6618

51. *Electrochem Commun* **2009**, 11, 1162-1165

52. *Electrochim. Acta* **2011**, 56, 6702-6708

53. Yu TH, Sha Y, Merinov BV, Goddard WA **2010**, *J Phys Chem C* 114:11527-11533

54. Wenpeng Li, Fu-Ren F. Fan, Allen J. Bard, *J Solid State Electrochem* **2012**, 16:2563-2568

55. S. J. Tauster, S. C. Fung, R. T. K. Baker, J. A. Horsley, Strong Interactions in Supported-Metal Catalysts, *Science* **1981**: Vol. 211, Issue 4487, pp. 1121-1125

56. Carmen Ocal, Salvador Ferrer, The strong metal support interaction (SMSI) in Pt-TiO₂ model catalysts, A new CO adsorption state on Pt-Ti atoms. *J.Chem.Phys.* **1986**, 84, 6474-6478

57. Shuyi Zhang, Philipp N. Plessow, Joshua J. Willis, Sheng Dai, Mingjie Xu, George W. Graham, Matteo Cargnello, Frank Abild-Pedersen, Xiaoqing Pan, Dynamical Observation and Detailed Description of Catalysts under Strong Metal-Support Interaction, *Nano Lett.* **2016**, 16, 4528-4534

58. Liang Wang, Jian Zhang, Yihan Zhu, Shaodan Xu, Chengtao Wang, Chaoqun Bian, Xiangju Meng, Feng-Shou Xiao, Strong Metal-Support Interactions Achieved by Hydroxide-to-Oxide Support Transformation for Preparation of Sinter-Resistant Gold Nanoparticle Catalysts, *ACS Catal.* **2017**, 7, 7461-7465

59. Qingying Jia, Shraban Ghoshal, Jingkun Li, Wentao Liang, Guannan Meng, Haiying Che, Shiming Zhang, Zi-Feng Ma, and Sanjeev Mukerjee, Metal and Metal Oxide Interactions and Their Catalytic Consequences for Oxygen Reduction Reaction, *J. Am. Chem. Soc.* **2017**, 139, 7893-7903

60. Tengfei Liu, Zengfeng Guo, Wenpeng Li*, Zongjie Pang, and Qingzhe Tong, Oxidation of Ethanol on Carbon-Supported Oxide-Rich Pd-W Bimetallic Nanoparticles in Alkaline Media, *Russian Journal of Physical Chemistry A*, **2017**, Vol. 91, No. 10, pp. 1994-2001

61. Zengfeng Guo, Tengfei Liu, Wenpeng Li*, Cai Zhang, Dong Zhang and Zongjie Pang, Carbon Supported Oxide-Rich Pd-Cu Bimetallic Electrocatalysts for Ethanol Electrooxidation in Alkaline Media Enhanced by Cu/CuOx, *Catalysts* **2016**, 6, 62

- 62. G. Staikov, Monte Carlo method, in: *ElectrocrySTALLization in Nanotechnology* Ch. 2.3, Wiley-VCH 2007
- 63. D.M. Kolb, G.E. Engelmann, J.C. Ziegler, On the unusual electrochemical stability of nanofabricated copper clusters, *Angewandte Chemie International Edition* 39 **2010**, 1123
- 64. *J Solid State Electrochem* **2012**, 16:2563–2568
- 65. *Electrochem Commun* **2009**, 11, 1162–1165
- 66. U. Holzwarth, N. Gibson, The Scherrer equation versus the 'Debye–Scherrer equation', *Nature Nanotechnology* 6 **2011**, 534
- 67. *Catalysts* **2016**, 6, 62; doi:10.3390/catal6050062
- 68. *Chinese Journal of Catalysis* 38 **2017**, 939–947
- 69. *Electrochimica Acta* 196 **2016**, 223–230
- 70. Yu TH, Sha Y, Merinov BV, Goddard WA **2010**, *J Phys Chem C* 114:11527–11533
- 71. W. Jung, J. Han, S. Ha, Analysis of palladium-based anode electrode using electrochemical impedance spectra in direct formic acid fuel cells, *Journal of Power Sources* 173 **2007**, 53.
- 72. P.J. Ferreira, G.J. la O', Y. Shao-Horn, Instability of Pt/C electrocatalysts in proton exchange membrane fuel cells, *Journal of The Electrochemical Society* 152 **2005**, A2256.
- 73. W.J. Wen, C.Y. Li, W.P. Li, Y. Tian, Carbon-supported Pd-Cr electrocatalysts for the electrooxidation of formic acid that demonstrate high activity and stability, *Electrochimica Acta* 109 **2013**, 201
- 74. D.A. Shirley, High-resolution X-Ray photoemission spectrum of the valence bands of gold, *Physical Review B* 5 **1972**, 4709